

MODELING MAGNETIC FIELDS FOR PRECISION MAGNETIC ACTUATORS THAT USE NON-PERIODIC MAGNET ARRAYS

Dariusz Golda¹ and Martin L. Culpepper¹
¹Department of Mechanical Engineering
Massachusetts Institute of Technology
Cambridge, Massachusetts USA

ABSTRACT

In this paper we use the Fourier transform (FT) to model and simulate the 3-D magnetic field created by finite, planar permanent magnet arrays that are Fourier-transformable and possess vertical magnetization. This approach captures the three dimensional characteristic of the fields, including the field components near the ends of the array. These end effects are important in small-scale precision actuators where geometric constraints preclude the use of larger, finite arrays that emulate the behavior of infinite arrays. We demonstrate how to model and compute the field characteristics using 2-D Fast Fourier transforms (FFTs). Model predictions for a prototype magnet array are compared with measured values of a magnet array's flux density. The difference between measured and predicted values is within the expected error (5%) of the measurement system.

INTRODUCTION

Permanent magnet arrays are important to precision actuators such as linear motors that use Halbach arrays [1, 2] and multi-axis magnetic levitation machines [3-5]. These devices often consist of long, repeating coils and permanent magnet arrays. In order to design such systems, infinitely periodic magnetic field models are used in performance models [1, 5]. However, meso-scale instruments and precision machines such as probe-based data storage systems [6, 7] employ non-periodic magnetic structures due to geometric constraints, and therefore modeling them requires a departure from conventional periodic field models. Meso-scale devices often include a set of permanent magnets that interact with an energized planar coil, as shown Fig. 1. In order to predict the performance of these actuators, non-periodic field models should be employed to capture end effects. Furthermore, accurate force models of these structures must consider field effects in three dimensions. This leads to a need to

develop accurate, yet computationally effective field models for the prediction of meso-scale magnetic actuator forces.

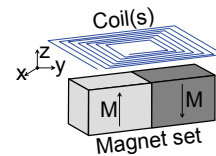


FIGURE 1: An actuator with a non-periodic array

The most commonly used method for modeling finite arrays, the superposition integral, only covers a limited number of array geometries and the equations become cumbersome for arrays of multiple magnets. In addition, the solution is unbounded along some of the magnet boundaries. For magnet-coil devices, the computation of the coil-field interactions in close proximity to the magnets requires fine discretization to ensure convergence. This is time and computationally intensive for design and optimization.

Herein, we demonstrate a new method that enables fast, accurate computation of the field components along a plane that is above or below a planar, non-periodic magnet array with vertical magnetization. This FT solution is well-suited to rapidly computing the forces on micro- or meso-scale planar coil actuators that are suspended above permanent magnet arrays. The advantages of this method over the superposition integral include:

- a) FFT algorithms are computationally more efficient than standard numerical integration methods;
- b) convergence is independent of distance from the pole surfaces, enabling small gaps without increased computation time;
- c) the resulting Fourier Transform integral field equations provide insight into the field solutions.

MODELING

Fig. 2 shows a schematic of the model that consists of a general, planar arrangement of permanent magnets with magnetization $M(x,y)$ that is directed in the vertical direction only. The magnitude and sign of this vector are free to vary in the x and y directions.

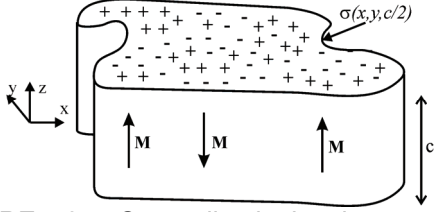


FIGURE 2: Generalized in-plane magnet arrangement with equivalent surface magnetic charge distribution $\sigma(x,y)$ at $z=\frac{1}{2}c$

Fig. 3 shows three regions of interest: regions 1 and 3 exist in air and extend to “infinity” above and below the array.

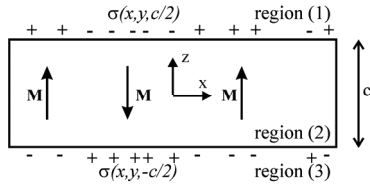


FIGURE 3: Side view of generalized charge distribution

Region 2 encompasses the magnet volume, extends to infinity in the x - y directions, and is bounded by the planes that define the upper/lower surfaces of the magnets. Under the magnetoquasistatic approximation [8] with zero current density, Maxwell’s equations for the field intensity, \mathbf{H} , and flux density, \mathbf{B} , simplify to:

$$\nabla \times \mathbf{H} = 0 \quad (1)$$

$$\nabla \cdot \mathbf{B} = 0 \quad (2)$$

As a result, the magnetic field, \mathbf{H} , is irrotational and may be expressed as the gradient of the scalar magnetic potential Ψ :

$$\mathbf{H} = -\nabla \Psi \quad (3)$$

The scalar potential satisfies Laplace’s equation subject to the boundary conditions imposed by the surface magnetic charge distribution [8]:

$$\sigma = -\mathbf{n} \cdot \mu_0 (\mathbf{M}_1 - \mathbf{M}_2) \quad (4)$$

In this paper, we provide an overview of the solution. For more details, see [9]. First, the charge distribution is expressed as a double inverse FT:

$$\sigma(x,y,c/2) = \frac{1}{(2\pi)^2} \int_{-\infty}^{\infty} \int_{-\infty}^{\infty} \Theta(k_x, k_y) \cdot e^{i(k_x x + k_y y)} dk_x dk_y \quad (5)$$

where Θ is the double FT of the surface magnetic charge distribution in the frequency domain. The solution is then derived by way of separation of variables and superposition. This leads to a solution in the form of a FT. The resulting magnetic field in each direction for all (x, y) in region 1 at a height z above the mid-plane of the magnet array is given as follows:

$$H_{1x} = \text{Re} \left[\frac{-i}{(2\pi)^2} \int_{-\infty}^{\infty} \int_{-\infty}^{\infty} \Theta(k_x, k_y) \frac{k_x}{k_{xy}} \cdot \sinh\left(k_{xy} \frac{c}{2}\right) e^{-k_{xy} z} e^{i(k_x x + k_y y)} dk_x dk_y \right] \quad (6)$$

$$H_{1y} = \text{Re} \left[\frac{-i}{(2\pi)^2} \int_{-\infty}^{\infty} \int_{-\infty}^{\infty} \Theta(k_x, k_y) \frac{k_y}{k_{xy}} \cdot \sinh\left(k_{xy} \frac{c}{2}\right) e^{-k_{xy} z} e^{i(k_x x + k_y y)} dk_x dk_y \right] \quad (7)$$

$$H_{1z} = \text{Re} \left[\frac{1}{(2\pi)^2} \int_{-\infty}^{\infty} \int_{-\infty}^{\infty} \Theta(k_x, k_y) \cdot \sinh\left(k_{xy} \frac{c}{2}\right) e^{-k_{xy} z} e^{i(k_x x + k_y y)} dk_x dk_y \right] \quad (8)$$

The field is a complex-valued function and therefore we only consider the real component. As long as the magnetic charge distribution is Fourier-transformable, the field may be calculated everywhere in three dimensions. It is typically difficult to directly calculate the integrals and therefore numerical solutions are useful. Several FFT algorithms have been developed to quickly compute FTs, and they may be used to perform fast computation of the fields along horizontal planes (constant z). We have shown that this method is computationally faster and has better accuracy than the superposition integral method [9].

EXAMPLE MAGNET ARRAY

An example array is used to illustrate the use of the field equations discussed above. The array consists of three alternating-pole magnets. The

magnet arrangement and parameters are shown in Fig. 4. The uniform magnetization, \mathbf{M} , is along the z direction, and a , b and c are the dimensions of the magnets. The coordinate system is located at the centroid of the center magnet, such that the charge surfaces are located at $z = \pm \frac{1}{2}c$ as in the preceding analysis.

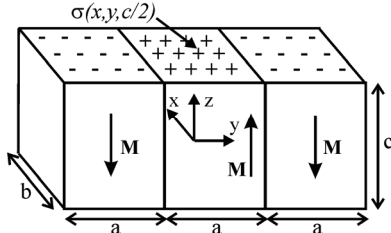


FIGURE 4: Schematic representation of the example 3-pole magnet arrangement

The arrangement of magnets in Fig. 4 has an even surface charge distribution function $\sigma(x,y, \frac{1}{2}c)$ that consists of three top-hat functions. The double FT of the distribution is:

$$\Theta(k_x, k_y) = \frac{4M}{k_x k_y} \sin \frac{1}{2} b k_y \left(2 \sin \frac{1}{2} a k_x - \sin \frac{3}{2} a k_x \right) \quad (9)$$

The model in Fig. 4 was used to predict the field characteristics for the array used in the following experiment.

COMPARISON OF THE PREDICTED AND MEASURED MAGNETIC FIELDS

An experimental setup was constructed to collect magnetic flux density data in three-axes, and upon a plane that was above an array of neodymium-iron-boron magnets. Fig. 5 shows the setup.

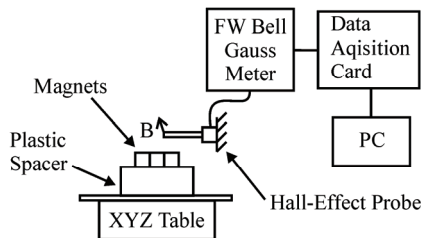


FIGURE 5: Schematic of the magnetic field measurement experiment

A set of the three permanent magnets was arranged according to Fig. 4 and then mounted on a programmable x - y - z translation table with positional accuracy of 12.7 micrometers. The magnet array was mounted to the table with a 100 mm plastic spacer to minimize field

interaction with the steel components of the translation table. A one-axis F. W. Bell Hall-effect probe (model HTG92-0608) was fixed above the magnet array and connected to an F. W. Bell Model 9550 Gauss meter. Total field measurement linearity error was less than 2%. Data from the Gauss meter was collected via a 12-bit National Instruments DAQCard-6024E PCMCIA card and a laptop PC running LabView. The system measurement noise floor was measured in regions of zero field to be 17.43 mT (95% confidence).

Measurements of independent flux density components were made by orienting the probe and stepping through a preset grid of x - y coordinates with pitch $p = 6.35$ mm. Measurements were taken at a fixed height, $h = 5.08$ mm, above the magnet's upper surface. The location of the magnet array was registered to the probe before making measurements by locating the maximum and zero-values of the flux density. The flux density components were recorded at each x - y coordinate, and the experiment was repeated for each field component, i.e. B_x , B_y and B_z . Table 1 lists the geometric and magnetic properties of the experiment.

TABLE 1. Experiment parameters

Symbol	Description	Quantity	Units
a	Magnet width	25.4	mm
b	Magnet depth	25.4	mm
c	Magnet height	25.4	mm
h	Height	5.08	mm
B_r	Remnance	1.23 ± 0.01	T
p	Pitch	6.35	mm

Nickel-plated N35-grade neodymium iron boron magnets were used in the experiment, and the catalog value for the remnance flux density was used in the calculations.

The predicted components were computed using a 2-D FFT algorithm. The $m \times n$ point FFT is computed for $m = n = 200$, or 40,000 total points. The corresponding truncation limits for K_x and K_y are $L = m\pi/12a \approx 2.06 \text{ mm}^{-1}$. Discretization of the magnetic charge distribution required approximately 1.5 sec, whereas calculation of all three field components along an $m \times n$ plane was approximately 0.15 sec. Figure 6A through 6C compare the measured and predicted components of the flux density.

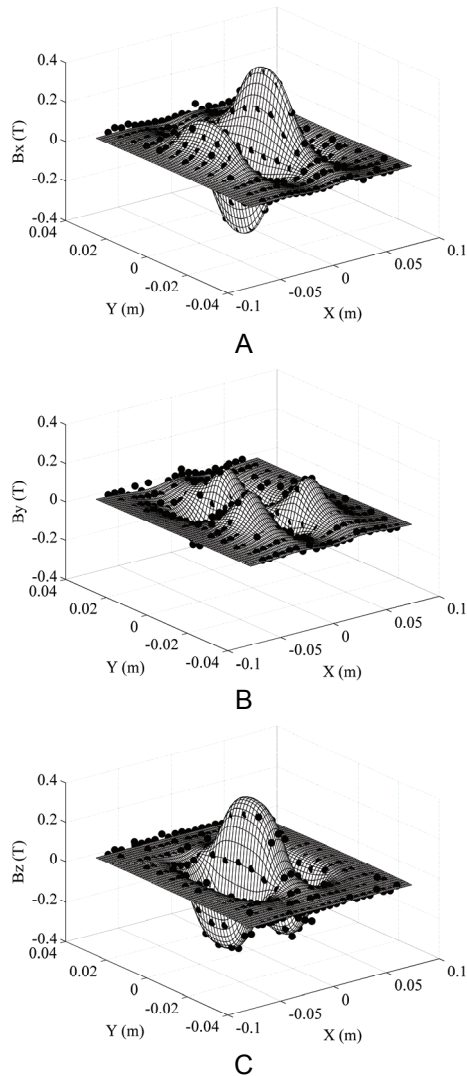


FIGURE 6: Comparison of predicted (surface) vs. measured (points) values of the x (A), y (B) and z (C) components of the magnetic flux density

The measurement error is at the system noise floor of 17.4mT, which is 4% of the maximum reading. The root-mean-square difference over the entire measurement grid is computed to be less than 5% of the maximum flux density value.

CONCLUSIONS

We use the FT to model and simulate the 3-D magnetic field created by finite, planar permanent magnet arrays that are Fourier-transformable and possess vertical magnetization. 2-D Fast FTs are used to quickly compute the fields in three-dimensions. Model predictions for a prototype magnet array are compared with measured values of a magnet array's flux density. The difference between

measured and predicted values is within the error (5%) of the measurement system. The FT solution is currently being used to design meso-scale actuators for high-speed six-axis nanopositioners.

ACKNOWLEDGEMENTS

This work is supported in-part by the National Science Foundation under Grant No. 0348242. We thank Prof. Jeffrey Lang and Prof. David Trumper for their modeling advice and access to measurement equipment.

REFERENCES

- [1] Trumper D L, et al. Magnet Arrays for Synchronous Machines. Proc. of the 28th IEEE Industry Applications Conf. Part 1 (of 3), Oct 3-8 1993, Toronto, Ont, Can, 1993.
- [2] Zhu Z Q, Howe D. Halbach Permanent Magnet Machines and Applications: A Review. IEE Proceedings-Electric Power Applications. 2001; 148: 299-308.
- [3] Compter I J C. Electro-Dynamic Planar Motor. Precision Engineering. 2004; 28:171-180.
- [4] da Silveira M A, et al. Evaluation of the Normal Force of a Planar Actuator. IEEE Transactions on Magnetics. 2005; 41:4006-8.
- [5] Cao J, et al. A Novel Synchronous Permanent Magnet Planar Motor and Its Model for Control Applications. IEEE Transactions on Magnetics. 2005; 41: 2156-63.
- [6] Choi J-J, et al. Electromagnetic Micro X-Y Stage for Probe-Based Data Storage. Journal of Semiconductor Technology and Science. 2001: 1: 84-93.
- [7] Rothuizen H, et al. Fabrication of a Micromachined Magnetic X/Y/Z Scanner for Parallel Scanning Probe Applications. Micro-electronic Engineering. 2000; 53: 509-12.
- [8] Haus H A, Melcher J R. Electromagnetic Fields and Energy. Prentice-Hall. Englewood Cliffs, NJ: 1989.
- [9] Golda D, Culpepper M L. Modeling 3D Magnetic Fields for Precision Magnetic Actuators That Use Non-Periodic Magnet Arrays. Accepted for publication in Precision Engineering, 2007.